Characterization of two ultraviolet–blue volume-phase holographic gratings based on dichromated gelatin and photopolymer recording materials

Alexandre Jeanneau, Andrea Bianco, Andrew Clawson, Michele Frangiamore, Elroy Pearson, Laurent Pinard, Jürgen Schmoll, Johan Richard, Rémi Giroud, Florence Laurent, et al.

▶ **To cite this version:**

Alexandre Jeanneau, Andrea Bianco, Andrew Clawson, Michele Frangiamore, Elroy Pearson, et al.. Characterization of two ultraviolet–blue volume-phase holographic gratings based on dichromated gelatin and photopolymer recording materials. Journal of Astronomical Telescopes Instruments and Systems, 2024, 10 (04), 10.1117/1.jatis.10.4.040501 . hal-04800804

HAL Id: hal-04800804
https://hal.science/hal-04800804v1

Submitted on 24 Nov 2024

HAL is a multi-disciplinary open access archive for the deposit and dissemination of scientific research documents, whether they are published or not. The documents may come from teaching and research institutions in France or abroad, or from public or private research centers.

L'archive ouverte pluridisciplinaire **HAL**, est destinée au dépôt et à la diffusion de documents scientifiques de niveau recherche, publiés ou non, émanant des établissements d'enseignement et de recherche français ou étrangers, des laboratoires publics ou privés.

JATIS Journal of Astronomical Telescopes, Instruments, and Systems

LETTER

Characterization of two ultraviolet–blue volume-phase holographic gratings based on dichromated gelatin and photopolymer recording materials

Alexandre Jeanneau,[a,*] Andrea Bianco,[b] Andrew Clawson,[c] Michele Frangiamore,[b] Elroy Pearson,[c] Laurent Pinard,[d] Jürgen Schmoll,[e] Johan Richard,[a] Rémi Giroud,[a] Florence Laurent,[a] and Roland Bacon[a]

[a]Université Lyon, Université Claude Bernard Lyon 1, Ens de Lyon, CNRS, Centre de Recherche Astrophysique de Lyon, Saint-Genis-Laval, France

[b]INAF – Osservatorio Astronomico di Brera, Merate, Italy

[c]Wasatch Photonics, Logan, Utah, United States

[d]Université Lyon, Université Claude Bernard Lyon 1, CNRS, Laboratoire des Matériaux Avancés, Villeurbanne, France

[e]Durham University, Centre for Advanced Instrumentation, Durham, United Kingdom

ABSTRACT. Volume-phase holographic gratings (VPHGs) are widely used in astronomical spectrographs due to their adaptability and high diffraction efficiency. Most VPHGs in operation use dichromated gelatin as a recording material, the performance of which is sensitive to the coating and development process, especially in the near-ultraviolet (UV). In this letter, we present the characterization of two UV-blue VPHG prototypes for the BlueMUSE integral field spectrograph on the Very Large Telescope, based on dichromated gelatin and the Bayfol®HX photopolymer film as recording materials. Our measurements show that both prototypes meet the required diffraction efficiency and exhibit similar performance with a wavelength-average exceeding 70% in the 350 to 580 nm range. Deviations from theoretical models increase toward 350 nm, consistent with previous studies on similar gratings. We also report similar performances in terms of spatial uniformity and grating-to-grating consistency. Likewise, no significant differences in wavefront error or scattered light are observed between the prototypes.

© 2024 Society of Photo-Optical Instrumentation Engineers (SPIE) [DOI: 10.1117/1.JATIS.10.4.040501]

Keywords: volume-phase holographic gratings; dichromated gelatin; photopolymer; diffraction efficiency; spectrograph; BlueMUSE

Paper 24092L received Jun. 20, 2024; revised Sep. 10, 2024; accepted Sep. 12, 2024; published Oct. 10, 2024.

1 Introduction

Volume-phase holographic gratings (VPHGs) operate through bulk refractive index modulations, which are created by holographically exposing a photosensitive material such as dichromated gelatin (DCG). Despite their widespread use in astronomical spectrographs over the past decades—owing to their adaptability and high diffraction efficiency[1,2]—the choice of VPHG suppliers is rather limited. This is partly due to the sensitivity of the DCG coating and development process,[3] particularly toward the near-ultraviolet (UV). Indeed, measurements of 36 VPHGs for the Dark Energy Spectroscopic Instrument suggest higher processing-induced

*Address all correspondence to Alexandre Jeanneau, alexandre.jeanneau@univ-lyon1.fr

2329-4124/2024/$28.00 © 2024 SPIE

efficiency variations in the UV–blue gratings with respect to other bands.[4] Measurements of four VPHG prototypes for the Visible Integral field Replicable Unit Spectrograph (VIRUS) reveal increasing efficiency deviations to the theoretical model toward 350 nm, which are attributed to process-induced absorption or scatter in the DCG layer.[5] However, Ref. 6 reported both minimal grating-to-grating scatter and minimal spatial variations toward 350 nm for the full suite of 170 VIRUS VPHGs.

Laminated self-processing photopolymers seem well suited to facilitate VPHG manufacturing and offer an increasingly broad range of thicknesses and achievable refractive index modulations.[7] This solution is particularly interesting for near-UV/visible instruments such as BlueMUSE[8] on the Very Large Telescope, which requires a high and consistent transmission across 16 replicated integral-field units.

In this letter, we compare two VPHG prototypes for BlueMUSE based on DCG and the Bayfol®HX photopolymer film[9] as recording materials. We assess manufacturing losses between modeled and measured diffraction efficiencies and cross-check characterization results provided by the manufacturers using an identical full aperture test setup. We also compare the transmitted wavefront error (WFE) as well as the bidirectional transmittance distribution function (BTDF).

2 Method

2.1 Manufacturing

Two VPHG prototypes are manufactured according to the design parameters listed in Table 1: the DCG-based prototype is manufactured by Wasatch Photonics, and another prototype based on the Bayfol®HX photopolymer is manufactured by the Osservatorio Astronomico di Brera (OAB). The DCG prototype was recorded with an exposure energy density of $\sim 75\ \mathrm{mJ/cm^2}$ at 515 nm, whereas the photopolymer-based grating required only $\sim 8\ \mathrm{mJ/cm^2}$ at 660 nm. The resulting gratings are shown in Fig. 1.

2.2 Diffraction Efficiency Test

Independent diffraction efficiency measurements have been carried out by Wasatch Photonics, OAB, and the Centre de Recherche Astrophysique de Lyon (CRAL). Unlike the setups at Wasatch Photonics and OAB, which rely on scanning a monochromatic test beam over the aperture and across the wavelength range, the method at CRAL is based on a full aperture test setup, shown in Fig. 2 and akin to the one described in Ref. 10. This choice was motivated by the desire to grasp diffraction efficiency variations over the clear aperture.

Briefly, the test beam is generated by a 150 W Xenon light source (Newport #6256 arc lamp) and filtered by a monochromator (Oriel Cornerstone CS130B) to a bandwidth of 4.5 nm varied

Table 1 Design parameters.

Design parameter	Value
Wavelength range	350 to 580 nm
Angle of incidence (AOI, in air)	13.72 deg ±0.7 deg
Line density	1027 ± 1 line/mm
Clear aperture	110 × 70 mm ellipse
Diffraction efficiency (excl. Fresnel losses)	$T(350\ \mathrm{nm}) \gtrsim 60\%$
	$T(580\ \mathrm{nm}) > 40\%$
	Goal: $T_{avg} > 70\%$
WFE (+1 order)	<1266 nm (2λ) PV
Substrate	Fused silica (uncoated)
Substrate size	130 × 90 mm

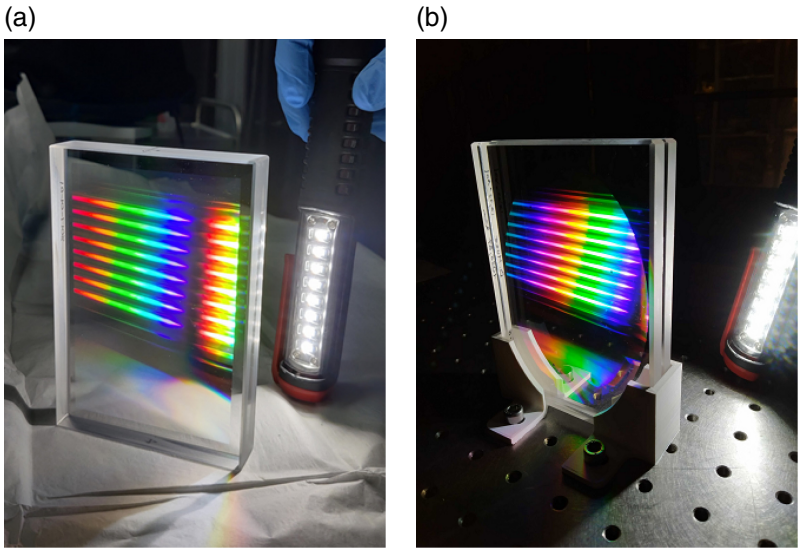

Fig. 1 DCG (a) and photopolymer (b) prototypes, back illuminated by a handheld lab light.

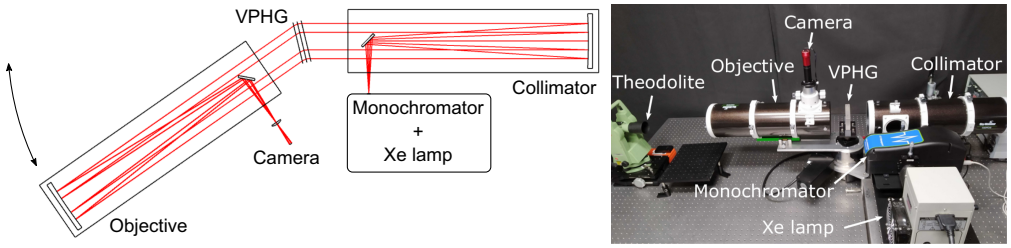

Fig. 2 Diffraction efficiency setup at CRAL.

from 330 to 600 nm. The beam is then directed toward a $f = 650$ mm—F/5 Newtonian telescope (Skywatcher Explorer 130PDS) used as a collimator. We mount the grating on a rotary stage and set it perpendicular to the collimated beam, using an autocollimation off the uncoated substrate. We establish this reference angle using a theodolite aligned with the monochromator slit. The grating is then rotated to the desired angle of incidence, and an identical telescope, used as an objective, is rotated as well to collect the diffracted light. A camera (ZWO ASI174MM 6 Mini) is placed after the telescope focus to image the grating clear aperture.

We divide the diffracted image by a reference image, where the grating is removed and both telescopes are aligned. To increase the overall S/N, we stack five exposures per diffracted and reference image. Finally, we mask out the region obstructed by the fold mirrors and spiders of the telescopes and smooth the resulting diffraction efficiency map using a 1×1 mm boxcar filter. Two diffraction efficiency maps are shown in Fig. 3. We assess the accuracy of this setup to $\sim 2\%$

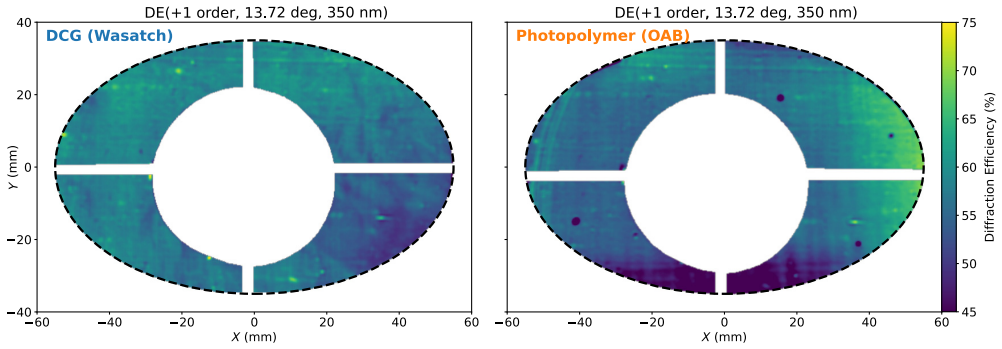

Fig. 3 Diffraction efficiency maps (AOI = 13.72 deg, $\lambda = 350$ nm). The region obstructed by the fold mirrors and spiders of the telescopes is masked out.

using repeated transmission measurements of an uncoated fused silica window. The setup is probably limited by straylight and lamp stability between the diffracted and reference images, which are separated by less than a minute.

3 Results

3.1 Diffraction Efficiency

Internal diffraction efficiency results (i.e., corrected for Fresnel losses) for unpolarized light are presented in Fig. 4. Both prototypes comply with the requirements presented in Sec. 2, albeit with different optimizations: the DCG prototype exhibits a lower average (72% versus 76%) but a better diffraction efficiency at 350 nm (62% versus 55%). We emphasize that the average diffraction efficiency and diffraction efficiency at 350 nm were given the same importance in the optimization of those prototypes, considering the combined impact of atmosphere cutoff and internal glass absorption on the overall transmission of BlueMUSE. We observe that measurements at CRAL agree with data from Wasatch Photonics and OAB to within 1% root mean square (rms).

We note that both prototypes almost reach the performance predicted by rigorous coupled-wave analysis (RCWA) models[11] at the red end but increasingly deviate toward the blue, particularly for the DCG prototype. The overall deviation for an angle of incidence of 13.72 deg is 23% for DCG and 12% for Bayfol®HX at 350 nm, compared with 9% and 7% on average, respectively. Finally, we find 16th to 84th percentile variations ($\pm 1\sigma$) of 6% across the clear aperture for DCG and 10% for Bayfol®HX at 350 nm, compared with 9% on average over the full wavelength range for both prototypes.

3.2 Wavefront Error

We measure the transmitted WFE in the 0th and $+1$ order using a Fizeau interferometer (4" Zygo Verifire XPD, $\lambda = 632.8$ nm) in a double-pass configuration, with the prototype set at its working angle and a $\lambda/25$ flat mirror closing the cavity. As the prototype clear aperture is slightly larger than the 4-inch test beam, we stitch three measurements per diffraction order. The resulting WFE maps are shown in Fig. 5. Both the DCG and photopolymer prototypes are well within the required WFE ($<2\lambda$ PV) with 451 nm PV (70 nm rms) and 523 nm PV (78 nm rms), respectively.

3.3 Scattering

Finally, we measure the BTDF in the dispersion direction and at the center of the clear aperture using a complete angle scatter instrument (TSW CASI scatterometer, Oregon City, Oregon, United States). The probe beam is an s-polarized HeNe laser with a ~1 mm spot diameter. The measured BTDF is shown in Fig. 6. Both prototypes have similar BTDFs within the limits of the probe beam signature, which spans ~10 BlueMUSE pixels compared with a slit width of 2 pixels. Therefore, this measurement mainly probes the outer scatter halo surrounding the point spread function.

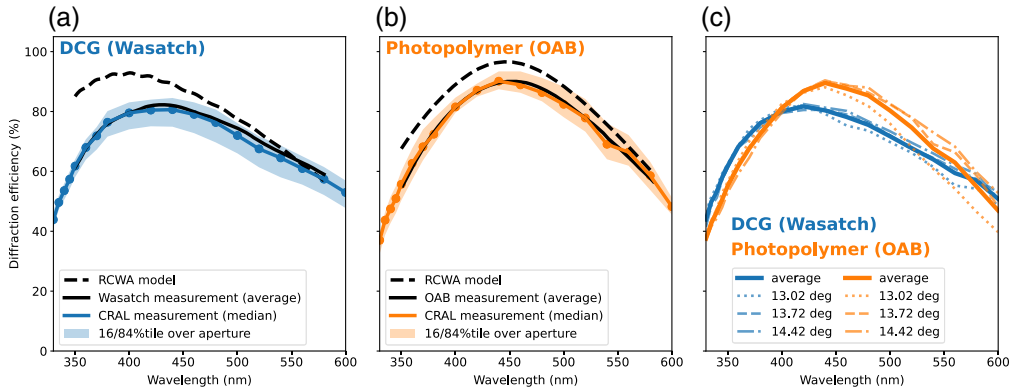

Fig. 4 Diffraction efficiency results: spatial uniformity of the DCG (a) and photopolymer (b) prototypes (AOI = 13.72 deg), and angular selectivity (c).

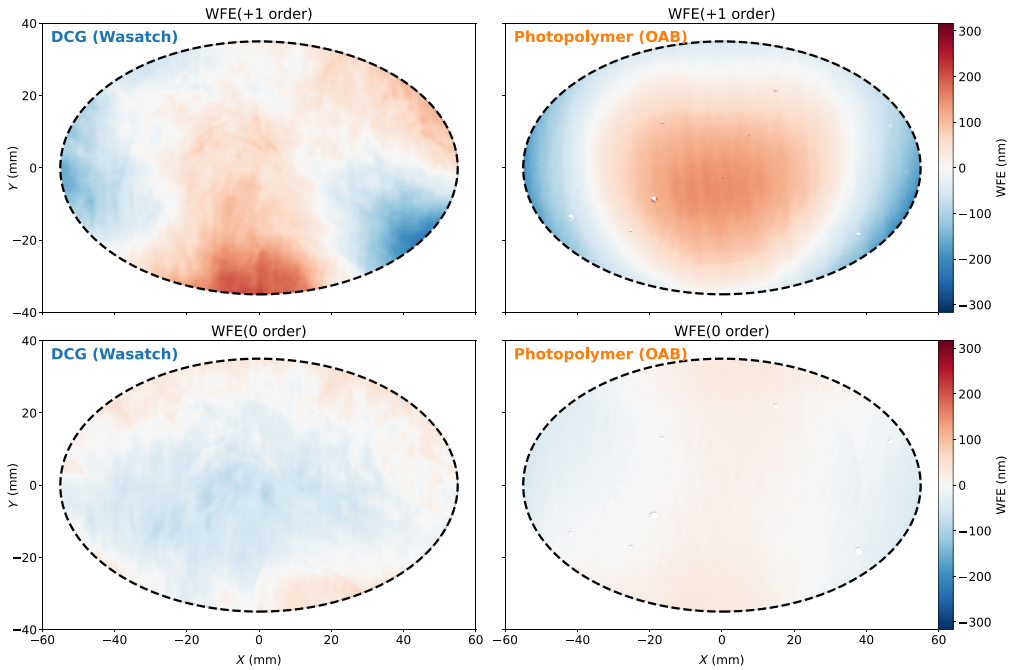

Fig. 5 WFE maps.

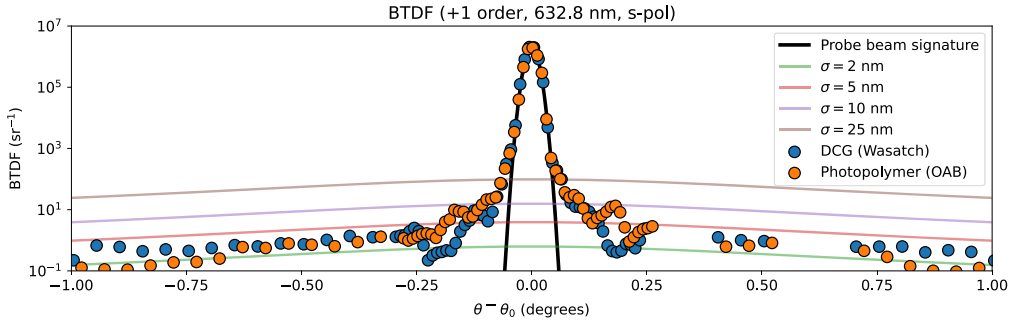

Fig. 6 Measured BTDFs in the dispersion direction, compared with the probe beam signature (black line) and models of smooth air-glass interfaces with varying microroughness (colored lines). Internal reflections at ~0.3 and ~0.6 deg are not shown.

4 Discussion

4.1 Diffraction Efficiency Uniformity and Consistency

Our measurements are consistent with expectations from Ref. 5, which reports increasing deviations from RCWA models toward the blue, with deviations up to 10% to 30% (~20% median) at 350 nm, for DCG-based gratings with a similar bandpass. According to Ref. 5, these deviations are likely due to processing-related absorption or scatter as they vary between production batches. The photopolymer prototype is at the lower end, with a 12% deviation at 350 nm, compared with a median value of 23% for the DCG prototype.

Although photopolymers are anticipated to provide more uniform performance across the clear aperture, our measurements show similar spatial variations for both the photopolymer and DCG prototypes. Notably, spatial variations above the median are smaller than those below the median, particularly for the DCG prototype. This aligns with Ref. 6, which attributes this to the higher likelihood of encountering a less favorable set of recording material properties (e.g., thickness or refractive index modulation) compared with the set optimized by design. Interestingly, the photopolymer prototype shows more balanced spatial variations around the median, even at peak diffraction efficiency (i.e., close to an optimal set of recording material properties). However, it is difficult to draw broad conclusions from a single realization of each manufacturing process.

To investigate grating-to-grating uniformity, OAB conducted a process repeatability test, recording and measuring four times a full aperture photopolymer film before encapsulation. The achieved diffraction efficiency demonstrated remarkable consistency, with wavelength-averaged variations of only 2%. For comparison, similar studies such as Refs. 4 and 6 reported grating-to-grating variations of 7% rms and 3% to 6% rms, respectively, for comparable but fully assembled DCG-based gratings. This consistency suggests that most of the spatial variations arise from very repeatable edge effects. Indeed, we observe that most of the efficiency variation is located at the edge of the clear aperture as in Ref. 4.

4.2 Wavefront Error

We note that the WFE in the 0th order is 3 to 4 times smaller than in the +1 order. This suggests that hologram recording errors are the primary contributors to the overall WFE, outweighing errors due to the substrate, recording material, or bonding, which tend to affect both orders similarly. In the photopolymer prototype, a significant portion of the diffracted WFE is due to a power term, which may be corrected during spectrograph alignment. This error likely arises from a slight collimation error in the recording beam.

4.3 Scattering

We approximate the measured straylight levels presented above by an equivalent surface microroughness, a useful quantity for generating simple yet realistic straylight models. We compare the prototypes against model BTDFs for smooth air-glass interfaces ($\Delta n = 0.5$) of varying microroughness ($\sigma = 2, 5, 10, 25$ nm), following the methodology of Ref. 12. We find an equivalent microroughness between 25 and 10 nm up to 0.10 deg, between 10 and 5 nm up to 0.25 deg, and below 5 nm for angles larger than 0.25 deg. This is a good straylight performance compared with the different grating technologies with similar line densities tested in Ref. 12, including a DCG-based VPHG, which reaches an equivalent microroughness below 5 nm for angles larger than 1.5 deg.

5 Summary and Conclusions

In this letter, we have compared two UV-blue VPHG prototypes developed for BlueMUSE, based on DCG and the Bayfol®HX photopolymer as recording materials.

1. We have presented a full aperture test setup at CRAL, which provides measurements in agreement to within 1% rms with respect to data from Wasatch Photonics and OAB.
2. Both prototypes comply with the required diffraction efficiency and achieve similar performance exceeding the wavelength-averaged goal of 70% over the BlueMUSE bandpass.
3. We observe that both prototypes increasingly depart from their RCWA model toward 350 nm, which confirms a trend reported in Ref. 5 for VIRUS prototypes.
4. Furthermore, we note that both prototypes have ~10% spatial efficiency variations. A repeatability test at OAB shows a remarkably consistent grating-to-grating performance with wavelength-averaged deviations of only 2%.
5. No significant differences in terms of WFE (<1λ PV) or scattered light are observed.

Although our measurements are based on a single realization for each manufacturing process, they offer valuable insights into the expected performance of the full suite of 16 VPHGs for BlueMUSE. Future statistical analyses of multiple photopolymer-based VPHGs will provide a more comprehensive understanding of the advantages and disadvantages of this recording material compared with DCG.

Disclosures

This letter is a revised version of a study submitted to SPIE Proceedings (#13100-210).

Code and Data Availability

Data are available from the authors upon reasonable request.

Acknowledgments

We acknowledge financial support from the Commission Spécialisée Astronomie Astrophysique (CSAA) of CNRS/INSU. We also acknowledge support from the FRAMA (Fédération de Recherche André-Marie Ampère) as well as the Labex-LIO (Lyon Institute of Origins) (Grant No. ANR-10-LABX-66) (Agence Nationale pour la Recherche).

References

1. S. C. Barden, J. A. Arns, and W. S. Colburn, "Volume-phase holographic gratings and their potential for astronomical applications," *Proc. SPIE* **3355**, 866–876 (1998).
2. S. C. Barden et al., "Volume-phase holographic gratings and the efficiency of three simple volume-phase holographic gratings," *Publ. Astron. Soc. Pac.* **112**, 809 (2000).
3. P.-A. Blanche et al., "Volume phase holographic gratings: large size and high diffraction efficiency," *Opt. Eng.* **43**(11), 2603–2612 (2004).
4. Y. Ishikawa et al., "Comprehensive measurements of the volume-phase holographic gratings for the Dark Energy Spectroscopic Instrument," *Astrophys. J.* **869**, 24 (2018).
5. T. S. Chonis et al., "Methods for evaluating the performance of volume phase holographic gratings for the VIRUS spectrograph array," *Proc. SPIE* **8446**, 84465H (2012).
6. T. S. Chonis et al., "Mass production of volume phase holographic gratings for the VIRUS spectrograph array," *Proc. SPIE* **9151**, 91511J (2014).
7. A. Bianco et al., "Improvements in VPHGs for astronomy based on photopolymers," *Proc. SPIE* **12574**, 125740H (2023).
8. J. Richard et al., "The Blue Multi Unit Spectroscopic Explorer (BlueMUSE) on the VLT: science drivers and overview of instrument design," *Proc. SPIE* **13096**, 1309622 (2024).
9. F.-K. Bruder, T. Fäcke, and T. Rölle, "The chemistry and physics of Bayfol® HX film holographic photopolymer," *Polymers* **9**(10), 472 (2017).
10. R. H. Barkhouser, J. Arns, and J. E. Gunn, "Volume phase holographic gratings for the Subaru Prime Focus Spectrograph: performance measurements of the prototype grating set," *Proc. SPIE* **9147**, 91475X (2014).
11. M. G. Moharam and T. K. Gaylord, "Rigorous coupled-wave analysis of planar-grating diffraction," *J. Opt. Soc. Am.* **71**, 811–818 (1981).
12. B. Harnisch et al., "Grating scattering BRDF and imaging performances: a test survey performed in the frame of the flex mission," *Proc. SPIE* **10564**, 105642P (2017).